CFD Analysis of Urban Climate in Kobe City : Application of nested grid technique to urban climate analysis

Ooka, Ryozo ; Murakami, Shuzo ; Mochida, Akashi ; Kim, Sangjin ; Naito, Kaori ; Moriyama, Masakazu ; Takebayashi, Hideki ; Shibaike, Hideki

(Citation)
神戸大学都市安全研究センター研究報告. 特別報告,1:271-278

(Issue Date)
1998-07

(Resource Type)
departmental bulletin paper

(Version)
Version of Record

(JaLCDOI)
https://doi.org/10.24546/00044742

(URL)
https://hdl.handle.net/20.500.14094/00044742

CFD Analysis of Urban Climate in Kobe City

Application of nested grid technique to urban climate analysis

Ryozo Ooka[1)] Shuzo Murakami[1)]
Akashi Mochida[2)] Sangjin Kim[1)]
Kaori Naito[1)] Masakazu Moriyama[3)]
Hideki Takebayashi[3)] Hideki Shibaike[4)]

Abstract : Urban climate in Kobe area is analyzed by 3D CFD simulation under typical summer conditions. The turbulence model developed by Mellor and Yamada (model level 2.5) is used for these simulations with hydrostatic assumption. Velocity and temperature distributions in Kobe area are given from the simulations. The agreement between the predicted results and the measurement is pretty good. Here, nested grid system is introduced in order to resolve the detailed distribution of land-use in Kobe with reasonable computational time and cost.

1. Introduction

We have developed the technique for modeling the physical phenomena related to an urban climate [1, 2]. An urban climate is highly influenced by differences in surface conditions and artificial heat releases. The effects of land-use and heat release on the urban environment have been investigated from various viewpoints by many researchers in the fields of meteorology, geography, city planning and building engineering using a one-dimensional (1D) boundary layer model [3, 4]. 1D analysis is seriously limited by 1D simplification since various flow phenomena peculiar to urban climate, such as heat island circulation etc., are highly three dimensional (3D). Thus these phenomena cannot be reproduced at all by 1D analysis. Therefore, 3D analysis is required for investigating the mechanism of urban climate.

This study investigates the urban climate in Kobe area with 3D CFD (Computational Fluid Dynamics) analysis. From a viewpoint of urban planning, it is important to consider various effects of land-use conditions on the urban environment. In many Japanese urban area and its surroundings, the topography and the land-use conditions are complicated. In particular, it is very complicated around Kobe city. This area is surrounded by mountainous area and the sea, and the shape of city itself is very long in east-west direction and very narrow in north-south direction. Furthermore, the land-use in Kobe city changes greatly position by position. Therefore, a high resolution of horizontal grid-discretization is required in order to investigate the detailed structure of the urban climate in Kobe city. On the other hand, the urban climate in Kobe area is strongly affected by larger scale meteorological phenomena. Thus, the size of computational domain should be large enough to reproduce the mesoscale climate in Kinki region accurately. This requires that the computational domain should cover approximately 300km×300km in horizontal direction, and 5km in vertical direction. Hence, a high grid-resolution implies a big computational load if we use an ordinary single grid system. The technique known as "nested grid", which has been successfully utilized in mesoscale weather forecasting, may be one of the solutions to fulfill the simultane-

ous requirements for fine grid resolution and a large computational domain [5, 6].

In this study, the urban climate in Kobe area is numerically investigated by using the three-dimensional CFD method, whose accuracy has been confirmed for the regional climate in the Kanto plain by the present authors. Furthermore, a nested grid technique is introduced and its availability is examined. Finally, some examples are presented for the possible contributions of CFD method to the urban planning.

2. Outline of Analysis

2.1 Model equations

Mellor and Yamada proposed a hierarchy of turbulence closure models for geophysical flow problems ranging from the 0 equation model (level 1) to the Differential Second-moment Closure Model (DSM, level 4) [7, 8]. This hierarchy of models was obtained by systematically simplifying the second-moment closure model. Their model level 2.5 was employed in this study [7]. This model corresponds to a simplified Algebraic Second-moment Closure Model (ASM) used in engineering field. All computations presented here were carried out by using HOTMAC (Higher Order Turbulence Model for Atmospheric Circulation) developed by Yamada and Bunker [6, 8]. In this study, various modifications were added to the original HOTMAC concerned with the initial condition of the mixing ratio of total water vapor, the boundary condition of evaporation from the ground, the value of albedo, etc. by the present authors. Boundary and initial conditions are described in Appendix 1.

2.2 Computational domain and computed cases

Figure 1 illustrates the computational domain (grid A), which covers 320km (east-west, x)×320km (north-south, y)×5km (vertical direction, z). The whole computational domain (grid A) is nested into two sub-domains ; grid B and grid C as is shown in Figure 1. Table 1 lists computed cases. In this paper, two cases of numerical

Table 1 Computed cases and grid discretization

computed case	grid system	computed domain	size (x)×(y)×(z)	grid discretization (x)×(y)×(z)	grid spacing in x and y directions
case1	single grid	grid A	320km × 320km× 5km	40×40×20	8km
case2	nested grid	grid A	320km × 320km× 5km	40×40×20	8km
		grid B	112km × 104km× 5km	28×26×20	4km
		grid C	64km × 56km× 5km	32×28×20	2km

Table 2 Surface parameters

land-use conditions	soil moisture availability β [9),10)]	albedo α	roughness length z_o (m)	artificial heat release (W/m^2)
Rice pad	0.5	0.2	0.05	0
Farming	0.3	0.1	0.01	0
Orchards	0.3	0.2	1	0
Orchards 2	0.3	0.2	0.5	0
Forest	0.3	0.15	2	0
Vacant land	0.3	0.2	0.01	0
Buildings	0	0.1	1	100
Paved road	0	0.1	0.01	4
Other land	0.3	0.2	0.01	0
River site	1.0	0.03	0.001	0
Coast	0.6	0.3	0.005	0
Ocean	1.0	0.03	0.001	0

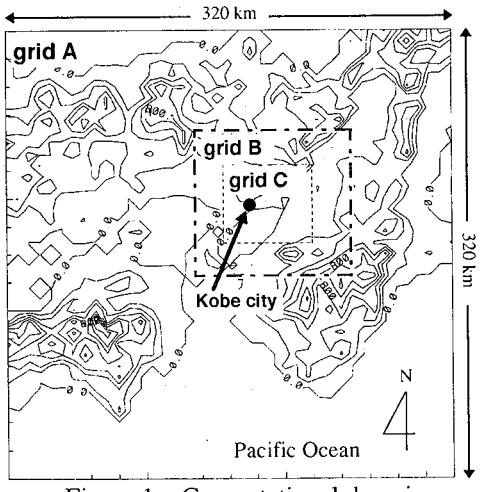

Figure 1 Computational domain

simulations are carried out. Case 1 is the computation with single grid system in which only grid A is used. Case 2 is the computation with all three grids, using the nested grid technique. The size and grid discretization of these sub-domain are shown in Table 1. In both cases grid spacing in z direction adjacent to the ground is set as 20 m.

In both cases, the conditions of land-use at present are incorporated into the computation. Here the ground surface is classified into 12 types of land-use , and surface parameters, such as albedo, roughness length, soil moisture availability β [9, 10] and artificial heat release are set individually following the land-use conditions as shown in Table 2. The present situation of land-use in Japan is given by utilizing the numerical data-base for land-use compiled by the National Land Agency of Japan [11]. The topography is also reproduced in both cases using this data-base. The daytime flowfield variations for these two cases are predicted by imposing the same initial conditions and the same boundary conditions at the outer surface of the computational domain, which are the typical meteorological conditions during early August in Japan.

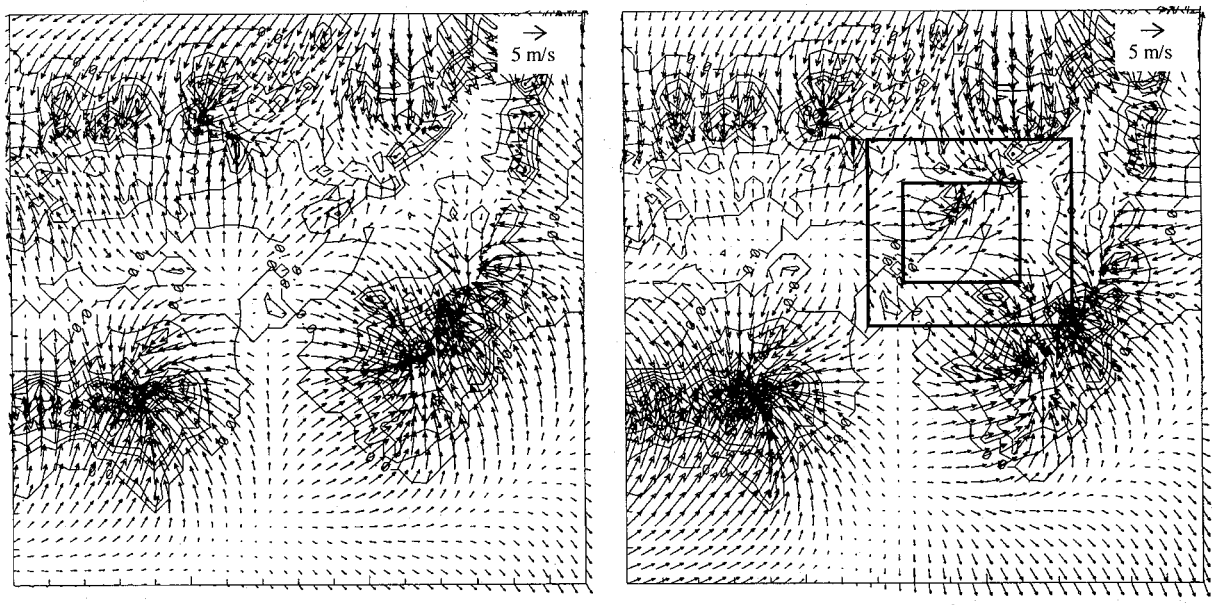

(1) case 1 (2) case 2

Figure 2 Wind velocity vectors in the whole domain (at 3:00 p.m. in early August at the height of 100m)

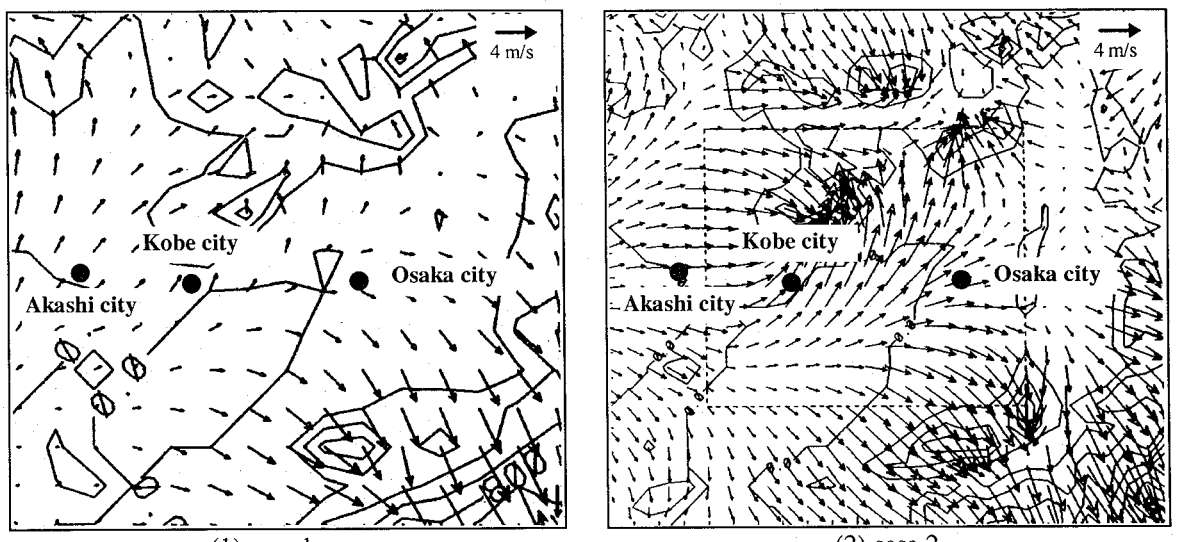

(1) case 1 (2) case 2

Figure 3 Wind velocity vectors in grid B (at 3:00 p.m. in early August at the height of 100m)

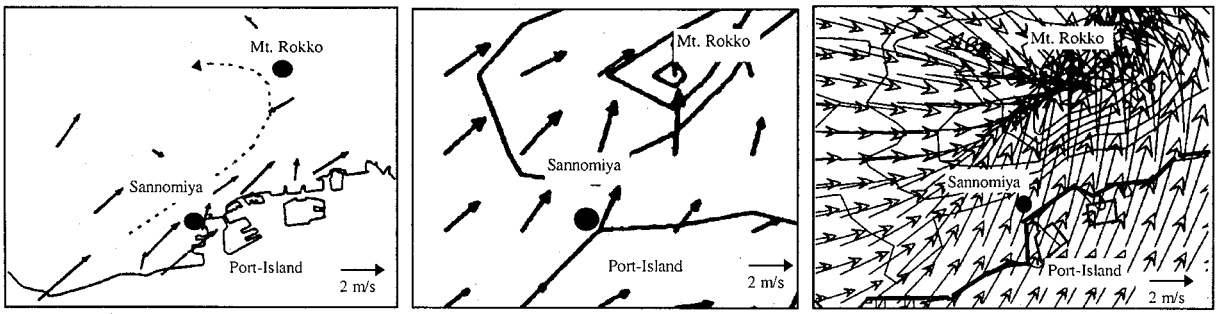

(1) measured data (2) case 1 (3) case 2

Figure 4 Wind velocity vectors inside Kobe city (at 3:00 p.m. in early August at the height of 100m)

3. Results and Discussion

Figure 2 shows wind velocity vectors at 100m height at 3:00 p.m. in early August which are the computed results after 33 hours from initial condition. The velocity vectors inside the grid B are also illustrated in Figure 3. In both cases, the flow pattern peculiar to sea breeze is well reproduced. The entire flow patterns are very similar for both cases, but some differences are observed between the results of cases 1 and 2 when we examine the velocity distributions in detail. For example, the wind directions that enter Osaka city and pass over Akashi city are different significantly between the two cases.

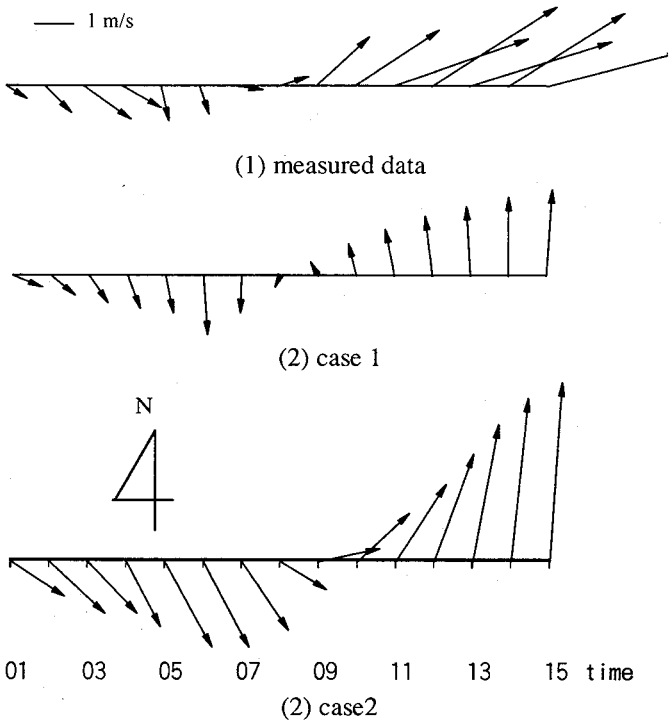

Figure 5 Diurnal variations of wind velocity vectors at Kobe city (in early August)

Figure 4 compares wind velocity vectors inside Kobe city for the same height and time as those for Figure 2. Figure 4(1) shows the measured data provided by Kobe City Atmospheric Monitoring Station which is the averaged value over the data of fine weather days in summer in 1990, 1991 and 1992. The height of measuring point is different at each Monitoring Station. Thus, the measured data in Fig.4(1) was obtained by extrapolating the measured one to the value at 100m height by assuming the logarithmic profile. The result of case 2 shows good agreement with the measurements in general (Fig.4(2)). The convergence of the flow toward Mt. Rokko is well reproduced in case 2, while this convergence is not observed in the result of case 1. The cause by which case 1 does not reproduce this convergence is attributed to smoothing effect with coarse grid used in case 1 (8km spacing in this case).

Figure 5 illustrates the diurnal variations of the wind velocity vectors at Kobe city. Figure 5(1) is the averaged value of the measured data of a meteorological observatory at Kobe city for 4 days (from 1st August to 4th August in 1995). Figures 5(2) and 5(3) show the results of cases 1 and 2 respectively. Both cases reproduce rather well the land breeze during the nighttime (north wind) and the sea breeze (south wind) during the daytime. In the measured data (Figure 5(1)), wind direction of land breeze at nighttime is NW or NWW and wind direction of sea breeze at daytime is SW or SWW. In the result of case 1 (Figure 5(2)), wind directions of land and sea

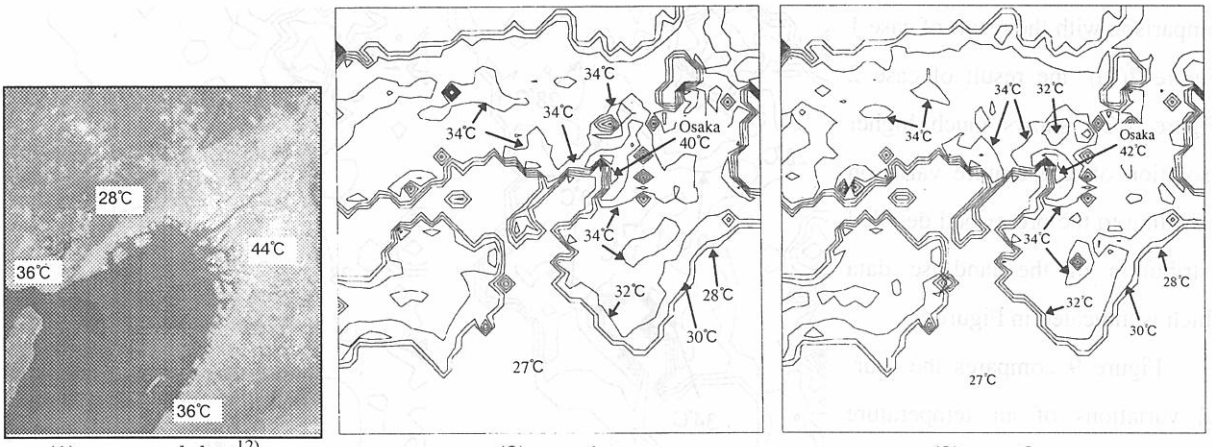

(1) measured data[12] (2) case 1 (3) case 2

Figure 6 Surface temperature distributions in grid A (at 3:00 p.m. in early August)

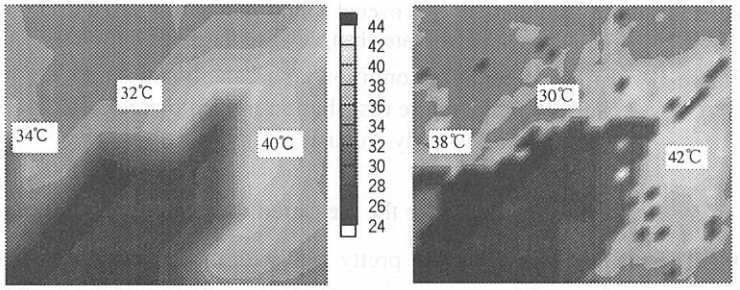

(1) case 1 (too much smoothed) (2) case 2

Figure 7 Surface temperature distributions in grid C (at 3:00 p.m. in early August)

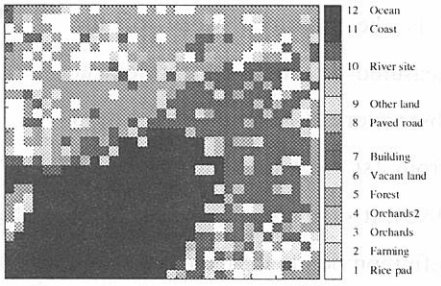

Figure 8 Land-use conditions in grid C

breeze are almost N and S respectively and some difference from the measurement is observed. On the other hand, in the result of case 2 (Figure 5(3)), wind directions of land and sea breeze are almost NW and SSW, thus the discrepancy of case 1 is corrected in some degree by introducing the nested grid. The agreement to the measurement in case 2 is fairly good. However we can see some overestimation of wind velocity at nighttime in case 2.

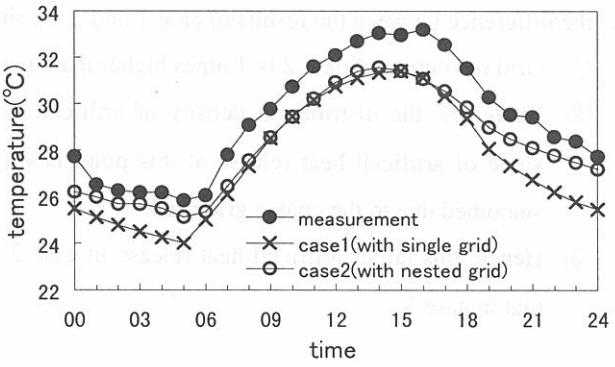

Figure 9 Diurnal variations of air temperature at Kobe city (in early August)

Table 3 Surface parameters at Kobe city

	soil moisture availability β	albedo	roughness length z_o(m)	artificial heat release (W/m^2)
case 1	0.34	0.12	0.88	15.8
case 2	0.39	0.15	0.81	41.06

Figure 6 shows surface ground temperature distributions at the same time with that of Figure 2. Figure 6(1) is the measured data derived from Landsat TM at 6th August 1990 [12]. The results of both cases (Figure 6(2) and Figure 6(3)) agree fairly well with the measured data. The peak value at Osaka city in case 2 is a little higher than that in case 1. Case 2 shows better agreement with the measured data.

As the nested grid system is adopted in case 2, the grid resolution inside this sub-domain (grid C) is 4 times higher than that in case 1. Figure 7 illustrates surface temperature distributions inside grid C at the same time. In

comparison with the result of case 1 (Figure 7(1)), the result of case 2 (Figure 7(2)) shows much higher resolution of temperature variation according to the prescribed detailed distribution of the land-use data which is indicated in Figure 8.

Figure 9 compares the diurnal variations of air temperature near the ground surface at Kobe city. The measured value in Figure 9 is the averaged value of the measured data of a meteorological observatory at Kobe city for 4 days (from 1st August to 4th August in 1995). It should be noted here that the height of measuring point is 1.5m for the measured data and the height of definition points for the computed cases is 10m. The results of case 2 agree pretty well with the measurement in nighttime. In this period (early August), a tropical night (minimum temperature in early morning exceeds 25℃) is observed in the measurement. The result of case 2 (nested grid) reproduces a tropical night fairly well, while that of case 1 (single grid) predicts air temperature near ground surface much lower at nighttime. The reasons which cause the difference between the results of case 1 and 2 are shown below.

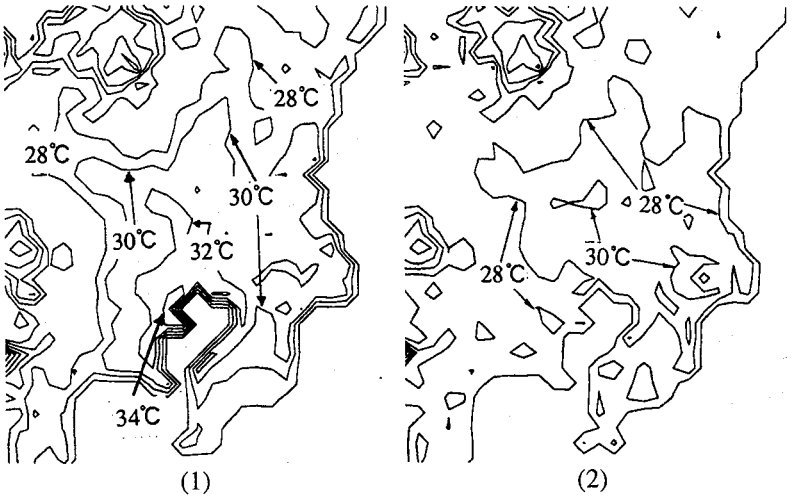

(1) (Surface boundary condition is given by the present land-use condition)

(2) (All surface parameters set in the areas covered with buildings and paved road are changed to be the value for forest)

Figure 10 Effect of land-use condition on urban climate (Surface temperature distribution in Kanto area at 3:00 p.m. in early August)

① Grid resolution of case 2 is 4 times higher than that of case 1 at Kobe city.

② Therefore, the distribution density of artificial heat release becomes much accurate in case 2. The value of artificial heat release at this point is very high (see Table 3). In case 1, this high value is smoothed due to the coarse grid used.

③ Hence, this larger artificial heat release in case 2 causes the higher air temperature at nighttime than that in case 1.

4. Prospects of CFD method for the use of urban planning

It is clarified that CFD method reproduces well the urban climate from the above discussion. The CFD method based on the physical modelling of urban meteorology has several advantages for the use for urban planning. From a viewpoint of urban planning, the most advantageous point of CFD method seems that it can predict effect of the change in land-use on the urban climate. For example, Figure 10 shows surface temperature distribution at 3:00 p.m. in early August in Kanto area under two different land-use conditions. Figure 10(1) is the result based on the present land-use condition near Tokyo area. Figure 10(2) is the result under the condition in which all buildings and paved road in computational domain are changed to forest. The surface temperature in the central part of Tokyo in Figure 10(2) decreases by about 4-5℃ compared with that in Figure 10(1). This means that the existence of forest produces a decrease of temperature in summer. The authors will carry out similar analysis

in Kobe area in the next stage.

5. Conclusion

1) 3D CFD analyses of the urban climate in Kobe area are presented. The results of the computations with single grid system and nested grid system correspond fairly well with measured data in general.
2) However, there are some differences between these two cases. The case with the nested grid system corresponds better with the measured data in various aspects compared to the case with single grid system.
3) The nested grid technique is a powerful tool for predicting physical phenomena related to an urban climate reflecting the detailed distribution of land-use.
4) From the example of CFD analysis in Kanto area, the CFD method can predict the effect of the change in land-use condition on the urban climate. This advantage will surely contribute to urban planning.
5) The authors will examine the effect of the change in land-use condition on the urban climate in Kobe city in near future.

Acknowledgment

The authors would like to express their gratitude to Dr. Tetsuji Yamada, Yamada Science and Art Corporation for his useful advice and comments.

Appendix 1

Surface heat energy balance The heat energy balance at ground surface is solved to impose the boundary conditions. The details are given in ref. [1].

Top and lateral boundary conditions At the top of the computational domain, U=0.13 m/s (velocity component in east-west direction), V=0.48 m/s (velocity component in north-south direction), $\Delta\Theta_v$=0, $Q_w \cong 0$, q^2=0, and l=0. The lateral boundary values for U, V, Θ, Q, q^2 and $q^2 l$ are obtained by integrating the 1D equations corresponding to the 3D transport equations for the variables, by imposing the condition that variations in the horizontal directions are zero. The soil temperature at 50 cm below the ground surface is set at 27℃ at Osaka. The water surface temperature is set from 25℃-29℃ inside the Osaka bay [13]. Outside the Osaka bay, the water surface temperature is set at 27℃.

Initial condition The initial wind direction is set south-west in the whole computational domain. Horizontal wind component V_s is assumed to be evaluated by the following formulas given by the similarity theory of Monin-Obukhov [1] from the ground up to the height where the wind speed reaches 0.5 m/s. Above this height, V_s is set to be constant (V_s=0.5 m/s). The vertical profile of potential temperature Θ_v is initially assumed to increase linearly with height according to the measurement of the Sionomisaki meteorological observatory at early August 1995. Initial potential temperatures are set homogeneous in horizontal directions. The initial relative humidity is set at 67% adjacent ground surface. The vertical profile of relative humidity is initially assumed to obey the equation of McClatchey [14]. Initial values for the mixing ratio of total water vapor at the ground are given by using the β method [1]. The initial conditions for turbulence kinetic energy $q^2/2$ and turbulence length scale l are given by solving the model level 2 proposed by Mellor and Yamada [7], in which distributions of $q^2/2$ and l

are calculated by algebraic expressions using the initial wind and temperature profiles.

Notation

V_s horizontal wind speed ($V_s = (U^2 + V^2)^{1/2}$)

Θ potential temperature ($\Theta = (P_o / P)^{R/Cp} T$)

Θ_v virtual potential temperature

Q_w mixing ratio of total water (vapor + liquid)

References

[1] A. Mochida, S. Murakami, T. Ojima, S. Kim, R. Ooka, H. Sugiyama, "CFD Analysis of Mesoscale Climate in the Greater Tokyo Area", *Computational Wind Eng.*(in press)

[2] Sangjin Kim, Shuzo Murakami, Akashi Mochida and Ryozo Ooka (1997) "CFD Analysis of Urban Heat Island in Tokyo :effects of land-use conditions on urban climate", *ICCCBE-7th*, NO.3, pp2111-2116.

[3] Atwater. M. A. (1972) "Thermal Effects of Urbanization and Industrialization in the Boundary Layer", *Boundary Layer Met.*, 3, pp.229-245

[4] M. Moriyama, M. Matsumoto (1988) "Control of Urban Night Temperature in Semitropical Regions During Summer" , *Energy and Buildings*, 11 pp.213-219

[5] F. Kimura (1984) "Numerical simulation of photo-chemical air-pollution using the local wind model", *Technical Reports of the Meteorological Research Institute* No.11, pp.217-296 (in Japanese)

[6] T. Yamada. and S. Bunker (1988), Development of a Nested Grid, Second Moment Turbulence Closure Model and Data Simulation", *J. of Applied Meteorology*, Vol. 27, 562-578.

[7] Mellor, G. L., and Yamada. T. (1974), "A Hierarchy of Turbulence Closure Models for Planetary Boundary layer", *J. of Applied Meteorology*, Vol. 13, No. 7, 1791-1806.

[8] T. Yamada. and S. Bunker. (1989), "A Numerical Model Study of Nocturnal Drainage Flows with Strong Wind and Temperature Gradients", *J. of Applied Meteo.*, Vol. 28, 545-554.

[9] H. Oue, H. Tagashira, K. Otsuki, and T. Maruyama (1993), "The Characteristics of Heat Balance and Temperature Regime in the Paddy, Potato, Bare Fields and in the Asphalt Area", *Trans. JSISRE*, 97-104.

[10] T. Fujino, C. Sibahara, T. Asaeda, N. Murase and A. Wake (1994), "Characteristics of Heat and Moisture Transport of permeable pavement", *Proceeding of Hydrol. Eng.*, Vol.38, 235-240.

[11] National Land Numerical Information (1992), "Planing and Coordination bureau", *National Land Information office.*

[12] M. Moriyama, K. Suzuki, H. Miyazaki (1996) "Thermal Environmental Evaluation for Wider Region in Summer Season using Land-sat TM", *J. Archit. Plann. Environ. Eng.*, AIJ, No.482, pp.51-56 (in Japanese).

[13] Osaka Prefectural Fisheries Experimental Station, "Annual Report of Osaka Prefectural Fisheries Experimental Station".

[14] McClatchey R.A, Fenn R.W., Selby J.E.A., Volz F.E., and Garring J.S.(1971), *AFCRL-71-0279*, No.354.

Authors 1) Institute of Industrial Science , University of Tokyo, 7-22-1, Roppongi , Minato-ku, Tokyo 106, Japan, 2) Niigata Institute of Technology, 1719, Fujihashi, Kashiwazaki, Niigata 945-11, Japan, 3) Research Center for Urban Safety and Security, Kobe University, Nada, Kobe 657, Japan, 4) Kyoto Institute of Technology, Matsugasaki, Sakyo-ku, Kyoto 606, Japan